



Energy, Mines and
Resources Canada

Énergie, Mines et
Ressources Canada

CANMET

Canada Centre
for Mineral
and Energy
Technology

Centre canadien
de la technologie
des minéraux
et de l'énergie

HYDROTREATING A DISTILLATE LIQUID FROM SUB-BITUMINOUS COAL
USING A SULPHIDED $\text{CoO} - \text{MoO}_3 - \text{Al}_2\text{O}_3$ CATALYST

M. Ternan and J.R. Brown

Catalysis Section
Synthetic Fuels Research Laboratories

ENERGY RESEARCH PROGRAM
ENERGY RESEARCH LABORATORIES
REPORT ERP/ERL 81-64(J)

ERP/ERL 81-64(J)

01-0003520

HYDROTREATING A DISTILLATE LIQUID DERIVED FROM SUB-BITUMINOUS COAL
USING A SULPHIDED $\text{CoO-MoO}_3\text{-Al}_2\text{O}_3$ CATALYST

by

Marten Ternan and James R. Brown

Energy Research Laboratories
Energy, Mines and Resources, CANMET
Ottawa, Ontario, K1A 0G1 Canada

SUMMARY

A coal derived heavy naphtha distillate containing 4.76, 0.51 and 0.004 mass percent oxygen, nitrogen, and sulphur respectively was hydro-treated. Even with severe processing conditions, the conversions of hetero-atom species were less than desired. An empirical equation based on the experimental data indicated greater conversions would be attained at greater pressures and residence time.

Severe catalyst deactivation was attributed to primarily carbonaceous deposits. However, smaller concentrations of zinc also accumulated on the catalyst.

INTRODUCTION

Several processes for hydrogenating coal to produce hydrocarbon fuels are being developed. When the product is to be used as a boiler fuel the desired specifications can often be obtained by the primary liquefaction process. When the final product is to be a transportation fuel such as gasoline, a secondary hydrotreating process is normally required. Sulphur, nitrogen and oxygen heteroatoms are removed by hydrotreating. For other products such as diesel fuel, conversion of aromatic compounds is also desirable during hydrotreating.

Catalytic hydrotreating (hydrocracking, hydrogenation, hydrodesulphurization, HDS, hydrodenitrogenation, HDN, hydrodeoxygenation, HDO, and hydrodemetallization, HDM) has been studied extensively and many studies on the subject have been published. Most of the work described in the literature was performed with either petroleum derived distillates or model compounds having relatively low molecular weights. In recent years the amount of work with higher molecular weight model compounds has increased. Studies have been published describing anthracene (1), phenanthrene and pyrene (2), perylene (3), 2-phenylnaphthalene (4), fluoranthene and chrysene (5), dibenzothiophene (6-12), acridine (13-15), benzoquinolines (16), and porphyrins (17). Data on HDO are less plentiful. Hydrotreating furan (18) and distillates from oil sand bitumen (19,20) have been described. Hydrocarbon liquids obtained from coal carbonization (21-24) and coal hydrogenation (25-30) have also been used. The hydrotreated coal liquids employed in the work referred to above tended to be of a higher molecular weight (e.g. solvent refined coal) than the coal derived fraction, containing naphtha, used in the work described here.

EXPERIMENTAL

The feedstock was obtained during a study of liquid fuel production from Canadian coals (31). Forestburg sub-bituminous coal was hydrogenated using a high pressure process, similar to the Bergius process developed in Germany during World War II (32). Processing conditions were 25 MPa, 465°C, 0.5 kg coal per hour per litre of reactor volume, and 0.268 kg H₂ per kg maf coal. For a catalyst, 1.9, 1.2, and 1.0% red mud, FeSO₄·7H₂O, and

$\text{Na}_2\text{S}\cdot 9\text{H}_2\text{O}$ were added respectively on an maf coal basis. Properties of the original coal and the hydrogenated liquid product are listed in Table 1.

Hydrotreating was performed using a Harshaw HT400 catalyst initially containing 15 mass percent MoO_3 and 3 mass percent CoO on gamma alumina. The catalyst was loaded into a fixed bed reactor having a volume of 155 mL and a length to diameter ratio of 12. It was sulphided at 400°C and atmospheric pressure in the presence of a flowing stream of hydrogen containing 10% H_2S . During the reaction experiments, the feedstock flowed continuously into the bottom of the reactor and up through the catalyst bed. Experiments were performed at pressures of 3.5-14 MPa, temperatures of $380\text{-}420^\circ\text{C}$, liquid space velocities of $1\text{-}4\text{ h}^{-1}$ and a hydrogen flow rate of 844 L hydrogen per L of feedstock (5000 scf/Bbl). The reaction system was maintained at steady state conditions for 1 h prior to and 2 h during the period in which the product was collected. The hydrotreated product was analyzed for carbon, hydrogen, and oxygen using a Perkin Elmer 240 analyzer. The sulphur was determined using the Wickbold technique and nitrogen by using a Dohrman microcoulometer. Samples were distilled chromatographically. Selected liquid products were analyzed using a Finnigan 4000 gas chromatography-mass spectrometry (GCMS) instrument having a INCOS data system. The surface of several samples of used catalyst were examined with a Physical Electronics model 548 x-ray photoelectron spectrometer (XPS), using Mg $\text{K}\alpha$ radiation. The instrument was calibrated using Au foil ($\text{Au } 4f_{7/2} = 83.8\text{ eV}$). The samples were examined as removed from the reactor, and after they had been Soxhlet extracted with benzene to remove any adhering oil.

RESULTS AND DISCUSSION

Figure 1 shows chromatographic distillation curves for the feedstock and for a product hydrotreated at 420°C , 13.9 MPa, and 1 LHSV. The distribution curve for the product has been shifted to lower temperatures by $15\text{-}20^\circ\text{C}$. Since this was one of the most severely hydrotreated products, it is apparent that excessive hydrocracking or molecular weight change did not occur.

Figure 2 shows the reconstructed ion chromatogram for the feedstock which was obtained by GCMS. Each of the peaks was identified. This was accomplished by examining the total mass spectra at a particular peak's reten-

tion time. It could be compared to fragmentation patterns for compounds stored in the computer library.

Reconstructed ion chromatograms for hydrotreated products were compared with the one for the feedstock, shown in Figure 2. The height of a peak in the product was divided by the height of the same peak in the feedstock. This provided a net indication of which components were being formed and which ones were being converted. Table 2 shows the relative amounts of n-alkanes. The group averages in Table 2 indicate that there was a net conversion of higher boiling n-alkanes to lower boiling n-alkanes. Presumably the amount of material in the n C15 - n C20 group would increase from the conversion of higher boiling components and decrease from conversion of components within its own group. The end result is that the quantity of material in this group remained approximately the same.

Table 3 shows the relative amounts of some condensed ring compounds. Two trends were observed for the aromatic ring compounds. First there is a general decrease in molecular weight. The four-ring aromatic compounds clearly decrease and the single ring components increase. Changes in two and three-ring compounds are smaller. Hydrogenation of aromatic rings is the second observed trend. On the basis of the relative amounts of the aromatic molecules shown in Table 3, a sequence of three general types of reactions can be suggested. Aromatic rings are hydrogenated. The hydrogenated aromatic ring is opened to form an alkyl side chain, attached to the parent ring structure. The alkyl side chain is completely or partially broken off the parent ring structure. The relative amounts of the various components in Table 3 support the above reactions, specifically the decrease in multi-ring aromatics, the increase in hydroaromatics and the increase in aromatics having alkyl chains attached. Not many oxygen containing compounds were identified by GCMS. The ones in Table 3 indicate that OH groups in phenol were removed but the oxygen atoms in furan were not.

The above discussion clearly indicates that paraffinic molecules are not predominant in the liquid product. The paraffins which are produced are of relatively low molecular weight. Therefore these hydrotreating conditions are not suitable for converting highly aromatic coal derived liquids into diesel fuel or other distillate fuels which require moderate aromatic contents. Perhaps some other combination of processes (possibly including Fischer Tropsch synthesis) will be required if paraffinic liquids are to be

obtained from coal.

Figure 3 shows some of the reaction results obtained at 13.9 MPa and 420°C using the raw data. Similar measurements were made at 400°C and 380°C. As anticipated the extent of reaction increased as space velocity decreased. The percent conversion for heteroatom removal increased in the order sulphur, nitrogen and oxygen. The order shown in Figure 3 is exactly opposite to the order of rate constants reported by Rollmann (18) for pure components. The validity of both sets of results can be explained.

The rates of reaction are proportional to the catalyst surface concentration of absorbed species. In turn the concentration of each adsorbed species will be related to its concentration in the bulk phase. If all reactions are first order in the concentration of the heteroatom species, each reaction rate will be equal to the product of the appropriate rate constant and the heteroatom species concentration. The conversions in Figure 3 are proportional to the concentrations of the heteroatom species in the feedstock. That is the oxygen concentration in the feedstock is greater than that of nitrogen which is greater than that of sulphur. Rollmann reported (18) that the rate constants varied in the opposite order. The validity of both sets of results can be explained by suggesting that in our study the variation of the heteroatom concentration has a greater effect than the variation of the rate constants. Specifically a very large oxygen concentration would offset a small oxygen removal rate constant. A very small sulphur concentration would offset a large sulphur removal rate constant.

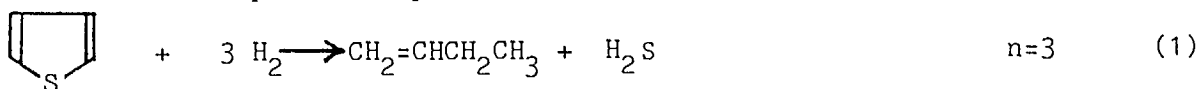
Figure 4 shows the hydrogen to carbon atomic ratio obtained at 13.9 MPa and different temperatures and space velocities. Although the data are scattered, it appears that hydrogenation decreases with increasing temperature. Even though reaction kinetics increase with increasing temperature, the equilibrium becomes less favorable for hydrogenation at higher temperatures.

The heteroatom conversions shown in Figure 3 are much lower than required. It would be desirable to know if processing conditions outside the range of values used here would produce improved conversions. Therefore the development of an empirical mathematical equation which represented the data was attempted. Hopefully conversions predicted by the equation at conditions not used experimentally would indicate trends which would be at least directionally correct.

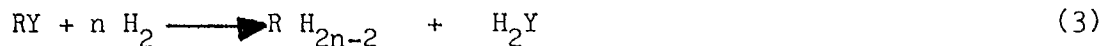
First the experimental data had to be adjusted to eliminate the effect of catalyst deactivation which was readily apparent. At each temperature, a series of experiments was performed at different space velocities, starting at 3 or 4 LHSV and decreasing to 1 LHSV. After the experiment at 1 LHSV was finished the first experiment at 3 or 4 LHSV was repeated. The change in conversion between the first and last experiments was an indication of the extent of catalyst deactivation.

An attempt to eliminate the effect of deactivation from the reaction data was made. The total amount of deactivation in each series of experiments was partitioned among each of the individual experiments performed. Thus, the experimental measurements were adjusted by progressively increasing amounts. That is experiments performed later in the sequence (when the catalyst was more deactivated) received larger adjustments than those performed near the beginning. For example, the amount of sulphur in the product liquid from the last experiment, in a series of experiments at constant temperature, was larger than from the first experiment. As mentioned above the first and last experiments in each temperature series were performed at identical processing conditions. If there were four experiments performed in a particular series, the difference in amount of sulphur between the first and fourth experiments was divided by three to obtain the sulphur increment. One sulphur increment would be subtracted from the amount of sulphur in the product liquid from the second experiment, two increments from the third experiment and three increments from the fourth experiments. In this way the results from the first and fourth experiment would be the same. All of the experimental data were adjusted in this way to obtain pseudo-undeactivated results which were considered to simulate results from fresh catalyst. In this way the raw data, such as those used to calculate the conversions in Figure 3, were adjusted. These pseudo-undeactivated results, were used to develop the empirical relationship which follows.

The number of molecules of hydrogen, n , which react with each molecule containing a heteroatom, varies. The stoichiometry for typical products from thiophene and phenol are examples:



The overall reaction for a molecule, RY, containing heteroatom Y can be written as:



If the elementary reaction had this stoichiometry, the reaction rate, r , could be written as:

$$r = \frac{-dC_{RY}}{dt} = k C_{RY} (p_{H_2})^n \quad (4)$$

where C_{RY} is the concentration of species RY, t is the reaction time or residence time in the reactor, and k is the rate constant. In reality rates of most elementary reactions (for example the reaction for the rate controlling step) will be first order in hydrogen pressure. It is unlikely that the elementary reaction will have the same stoichiometry as the overall reaction if the value of n is greater than one. Equation 4 can be rearranged for integration.

In flow experiments, p_{H_2} can be maintained constant so that its variation with reaction time and concentration of species RY will be small. After integration Equation 4 becomes

$$\ln \left(\frac{C_{RYo}}{C_{RY}} \right) = k (p_{H_2})^n \theta_M \quad (5)$$

where C_{RYo} is the initial concentration of species RY and θ_M is the mean residence time in the reactor. The conversion, X , of the heteroatom species can be approximated by

$$X = \frac{C_{RYo} - C_{RY}}{C_{RYo}} \quad (6)$$

which upon rearrangement becomes

$$\frac{C_{RYo}}{C_{RY}} = \frac{1}{1 - X} \quad (7)$$

When a series of experiments are performed at the same pressure

$$k' = k (p_{H_2})^n \quad (8)$$

Equations 7 and 8 can be substituted in Equation 5 to obtain

$$\ln \frac{1}{1 - X} = k' \theta_M \quad (9)$$

The conversion data obtained at 13.9 MPa in the form of the left hand side

of Equation 9 can be plotted against residence time. The data should fall on a straight line having slope k' . Figure 5 shows the nitrogen data in this format. Unfortunately the straight lines do not go exactly through the origin. The deviation from the origin was greatest for the hydrodeoxygenation results. Therefore an empirical constant, b , was added to Equation 9 to represent the straight line.

$$\ln \frac{1}{1-X} = k' \theta_M + b \quad (10)$$

This equation indicates that there is a certain amount of conversion that occurs at zero residence time, which is physically impossible. The physical significance of the constant b can be explained in terms of the feedstock being a mixture rather than a single component. Some of the components in the mixture react readily. At higher conversions, to be predicted by Equation 10, the rate will be controlled by species which react more slowly. The value of b is related to the conversion of components which react readily.

The rate constants obtained from Equation 10 were used in the Arrhenius equation,

$$\ln k' = \ln A - E/RT \quad (11)$$

where A is the Arrhenius pre-exponential factor, E is the activation energy and R is the gas constant. Figure 6 shows the data plotted in this manner. Pre-exponential factors and activation energies obtained from Figure 6 are listed in Table 4. The activation energies in Table 4 are of the same order of magnitude as those reported by Qader, Wiser and Hill (21).

The empirical equation used for the predictions was obtained by substituting equation 8 (with $n=1$) and the exponential form of Equation 11 into Equation 10 to obtain

$$\ln \frac{1}{1-X} = A [\exp(-E/RT)] (p_{H_2}) (\theta_M) + b \quad (12)$$

Predictions were made for HDS, HDN and HDO using equations of the form of Equation 12 and the parameters given in Table 4. These predictions are compared with data obtained at various pressures in Figure 7. It is apparent that the data does predict a decrease in conversion with decreasing pressure. This is consistent with the data.

Conversions that would be obtained on fresh catalysts, were also

predicted at processing conditions outside the range of variables used in the experiments. These results are shown as a function of temperature, pressure and residence time in Figure 8 for HDS, Figure 9 for HDN and Figure 10 for HDO. As expected, they indicate better conversions at higher pressures. However, reasonably good improvements are also predicted at longer residence times. These figures suggest that much more severe hydrotreating conditions are required for this feedstock than for petroleum fractions of similar boiling range.

As mentioned previously the catalyst fouled rapidly. The fouling was observed by monitoring changes in the properties of the product with increasing time on stream. Changes in specific gravity of the product from this coal derived liquid are compared with those from a 345-525°C gas oil and from Athabasca bitumen in Figure 11. The gas oil and bitumen results were obtained by operating the reactor at the same conditions for relatively long periods of time. With the coal derived liquid, experiments were run at many different conditions. However certain experiments were repeated at intervals to indicate deactivation. The change in specific gravity provided an index of the catalyst deactivation.

The comparisons in Figure 11 are obviously qualitative. The 50-400°C coal derived liquid has a lower boiling range than the 345-525°C gas oil, yet it causes much more rapid catalyst deactivation. The deactivation is comparable to Athabasca bitumen which is normally considered to have a large propensity to form coke, as measured by Conradson Carbon residue (13.3 m%) and pentane insolubles (15.5 m%). The values of these properties for the coal derived liquid, listed in Table 1 are much lower. The catalyst coke content after processing the coal derived liquid was $0.737 \text{ mg C m}^{-2}$, which is equivalent to 1.8 statistical monolayers. This compares to 1.1 statistical monolayers obtained in a similar experiment with bitumen (33). It is likely that catalyst deactivation from carbonaceous deposits is primarily caused by heteroatoms being chemisorbed by the electron acceptor sites on the alumina portion of the catalyst. Furimsky (34) has extracted the used catalyst pellets with different solvents and found the O:C and N:C ratios to be higher in the extracts than in the coal derived liquid feedstock.

An X-ray photoelectron spectroscopy (XPS) study of the deactivated catalyst surface indicated that zinc had been deposited. A comparison of

fresh and used catalysts is shown in Table 5. The presence of zinc on the surface of the used catalyst is clearly evident. A large sample of the coal liquid feedstock was ashed and the ash analyzed to see if the zinc originated in the liquid. The sample (total ash content 0.05 mass %) was drawn from just below the top of the liquid surface in a barrel which had not been moved for several months. This was done to ensure that the sample did not contain any solids which might have settled at the bottom of the barrel. The ash analysis of the used catalysts shown in Table 5 indicated considerable zinc. It is likely that zinc containing organo-oxygen complexes are present in the liquid. Some of these complexes are likely destroyed when H₂O occurs at the catalyst surface. The zinc would then precipitate onto the catalyst surface.

The zinc probably originates in the red mud which was one of the catalytic agents used in the primary coal hydrogenation process. Red mud is a by-product of an alumina refining process which uses bauxite as a raw material. Zinc is known to be one of the minor components in European bauxites.

The hydrotreated coal derived liquid products also contained Na₂SO₄ solids. This probably originated from the Na₂S which was added as the catalyst during the primary hydrogenation process, used to produce the coal derived liquid. Sodium was not found deposited on the catalyst surface. This suggests that the sodium species were present as particulate matter and not organometallic complexes which were later decomposed and deposited at the catalyst reaction site.

The conclusions of this work may be summarized as follows. The conversions of heteroatom species were lower than those generally required. The experimental data were used to develop an empirical equation which indicated greater conversions would be obtained by increasing hydrogen pressure and residence time. The rapid catalyst fouling was attributed to two factors. The formation of carbonaceous deposits was considered to be enhanced by nitrogen and oxygen heteroatom species adsorbing at electron acceptor sites in the alumina catalyst support. Zinc, originating in the red mud primary coal hydrogenation catalyst, may have formed organometallic complexes with the feedstock which were later decomposed on the secondary hydrotreating catalyst used in this study. Three generalizations can be made. Severe hydrotreating conditions are required for heteroatom removal from

this coal derived liquid. Hydrotreating converts polyaromatic molecules into aromatic molecules with fewer rings plus low molecular weight paraffins. Conversion of aromatic molecules does not result in paraffins of equivalent molecular weight so that hydrotreating is not a suitable process for producing diesel fuel with a high cetane number from highly aromatic feedstocks.

ACKNOWLEDGEMENT

The authors would like to acknowledge the contribution of E.C. McColgan who performed the hydrotreating experiments and P.L. Lafontaine who performed the GCMS measurements.

REFERENCES

1. Cowley, S.W. and Wiser, W.H., Fuel Proc Technol 2, 317; 1979.
2. Shabtai, J., Veluswamy, L. and Oblad, A.G. "Steric effects in Phenanthrene and pyrene hydrogenation catalyzed by sulphided Ni-W/Al₂O₃; Preprints, Fuel Chem, Am Chem Soc 23(1), 107; 1978.
3. Dekker, J., Nell, B.C.K. and Potgieter, H.G.J., Fuel 57 361; 1978.
4. Sapre, A.V. and Gates, B.C., Ind Eng Chem Proc Des Dev 20, 68; 1981.
5. Nakatsuji, Y., Kubo, T., Nomura, M. and Kikkawa, S. Bull Chem Soc; Japan 51, 618; 1978.
6. Bartsch, R. and Tanielian, C. J Catal 35, 353 (1974), J Catal 50, 35 (1977).
7. Sternberg, H.W., Donne, C.L.D., Markby, R.E. and Friedman, S. Ind Eng Chem Proc Des Dev 13, 435; 1974.
8. Nagai, M., Urimoto, H. and Sakikawa, N. Nippon Kagaku Kaishi (No. 2), 356; 1975.
9. Houalla, M., Brodenick, D., de Boer, V.H.J., Gates, B.C. and Kwart, H. "Hydrodesulphurization of Dibenzothiophene and related compounds catalyzed by sulphided CoO-MoO₃- α -Al₂O₃ effects of reactant structure on reactivity"; Preprints, Petrol Chem, Am Chem Soc 22(3), 941; 1977.
10. Klemm, L.H. and Karchesy, J.J. J Heterocycl Chem 15, 65; 1978.
11. Dhainaut, E., Gachet, C. and deMourgues, L. C.R. Hebd. Seances, Acad Sci Series C; 288, 339; 1979.
12. Geneste, P., Amblard, P., Bonnet, M. and Graffin, P. J Catal 61, 115

(1980).

13. Shih, S., Reiff, E., Zawadzki, R. and Katzer, J.R. "Effect of catalyst composition on quinoline and acridine hydrodenitrogenation; Preprint, Fuel Chem, Am Chem Soc 23(1), 99; 1979.
14. Katzer, J.R. and Sivasubramanian, R., Catal Rev Sci Eng 20(2), 155; 1979.
15. Cocchetto, J.F. and Satterfield, C.N., Ind Eng Chem Proc Des Dev 15, 272; 1976.
16. Shabtai, J., Veluswamy, L and Oblad, A.G. Preprints, Fuel Chem, Am Chem Soc 23(1), 114; 1978.
17. Hung, C.W. and Wei, J., Ind Eng Chem Proc Des Dev 19, 250; *ibid* p 257; 1980.
18. Rollmann, L.D., J Catal 46, 243; 1977.
19. Furimsky, E. Fuel 57, 494; 1978.
20. Furimsky, E. AIChE J 25, 306; 1979.
21. Quader, S.A., Wisler, W.H. and Hill, G.R., Ind Eng Chem Proc Des Dev 7, 390; 1968.
22. Quader, S.A. and Hill, G.R., Ind Eng Chem 8, 462; 1969.
23. Qader, S.A. and Hill, G.R., Fuel 51, 54; 1972.
24. Qader, S.A. and Hill, G.R. "Development of catalysts for the hydrocracking of polynuclear aromatic hydrocarbons"; Preprints, Fuel Chem, Am Chem Soc 16(2) 93; 1972.
25. Sivasubramanian, R. and Crynes, B.L., Ind Eng Chem Prod Res Dev 19,

456; 1980.

26. Lovetro, D.C. and Weller, S.W., Ind Eng Chem Proc Res Dev 16, 297; 1977.
27. Satterfield, D., Lanning, W.C. and Poyer, R.E. "Hydrotreatment and biological test of SRC II coal liquid"; Preprints, Fuel Chem, Am Chem Soc 25(1), 79; 1980.
28. Sivasubramanian, R., Olson, J.H. and Katzer, J.R. "Catalyst deactivation in hydrotreating coal-derived liquids"; Preprints, Fuel Chem, Am Chem Soc 25(1), 85; 1980.
29. Berg, L., and McCandless, F.P. "Catalytic hydrogenation of coal derived liquids"; FE-2034-18, NTIS, March 28, 1980.
30. Swager, I. Development of new catalysts for coal liquids refining"; FE-2595-5, NTIS, April 1980.
31. Kilborn Alberta Limited, "Coal liquefaction plant feasibility study"; Supply and Services Canada, Contract No. 18 SQ-23440-8-9125-4.
32. Wurfel, H.E., Fuel Proc Technol 2, 227; 1979.
33. Ternan, M., Furimsky, E. and Parsons, B.I., Fuel Proc Technol 2, 45; 1979.
34. Furimsky, E. "Characterization of deposits formed on catalyst surfaces during hydrotreatment of coal derived liquids"; Fuel Proc Technol. (accepted for publication).



CAPTIONS

- Figure 1 Chromatographic distillation volume percent distilled versus temperature ($^{\circ}\text{C}$).
- Figure 2 Reconstructed ion chromatogram intensity versus retention time (min).
- Figure 3 Hydrogen to carbon atomic ratio and conversion of heteroatoms (mass percent) versus liquid hourly space velocity (h^{-1}).
- Figure 4 Hydrogen to carbon atomic ratio versus temperature ($^{\circ}\text{C}$) at various liquid hourly space velocities (h^{-1}).
- Figure 5 Natural logarithm $1/(1 - X)$ versus reactor residence time (s) for hydrodenitrogenation squares, circles and triangles are for 420, 400 and 380 $^{\circ}\text{C}$ respectively.
- Figure 6 Natural logarithm of the first order rate constant, k , versus inverse temperature (K^{-1}). Triangles, circles, and squares represent, hydrodenitrogenation, hydrodeoxygenation, and hydrodesulphurization respectively.
- Figure 7 Conversions (mass fractions) versus pressure (MPa). Circles, squares, and triangles are experimental points for oxygen, nitrogen and sulphur removal respectively. The dotted lines were predicted from Equation 12.
- Figure 8 Predicted hydrodesulphurization (HDS) conversion (mass fraction) versus mean residence time (θ_M) at various temperatures.
- Figure 9 Predicted hydrodenitrogenation (HDN) conversion (mass fraction) versus mean residence time (θ_M) at various temperatures.

Figure 10 Predicted hydrodeoxygenation (HDO) conversion (mass fraction) versus mean residence time (θ_M) at various temperatures.

Figure 11 Decrease in liquid product specific gravity versus catalyst time on stream for 345-525 gas oil, Athabasca bitumen, and the coal derived liquid used in this study.

Table 1 - Feedstock Properties

	Forestburg Coal Sub-bituminous C mass %	Hydrogenated Liquid mass %
<u>Proximate Analysis</u>		
Moisture	17.2	
Ash	10.7	
Volatile matter	31.1	
Fixed carbon	41.0	
<u>Ultimate Analyses</u>		
Carbon	53.1	85.32
Hydrogen	3.5	9.64
Sulphur	0.9	0.084
Nitrogen	1.0	0.51
Ash	10.7	0.057
Oxygen (by diff.)	13.6	-
Oxygen (measured)		4.76
Water	17.2	0.4
Pentane insolubles		0.46
Conradson carbon		0.59
Amount Distilled at Temp.		
101°C		10
216°C		50
310°C		90
<u>Maceral Composition</u>		
Vitrinite	86.6	
Exinite	1.9	
Semi-fusinite	2.1	
Fusinite	2.5	
Micrinite	2.9	
Mineral matter	4.0	

Table 2 - Relative amounts of n-Alkanes

n-Alkane	Relative Amount		Group Average
	Product	Feed	
n C8		1.15	
n C9		1.0	
n C10		1.12	1.14
n C11		1.23	
n C12		1.14	
n C13		1.18	
n C15		1.03	
n C17		0.97	
n C18		1.0	1.02
n C19		0.93	
n C20		1.15	
n C21		0.65	
n C22		0.53	
n C23		0.38	0.42
n C25		0.30	
n C26		0.22	
n C27		0.43	

n C14, n C16, n C24 species had the same retention time as other components and were not identified separately

TABLE - 3

PRODUCT QUANTITY/REACTANT QUANTITY: FOR SEVERAL COMPOUNDS

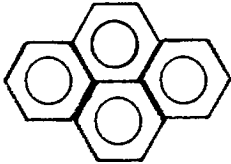
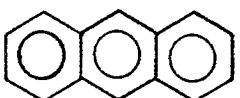
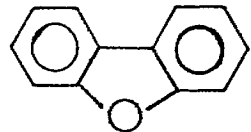
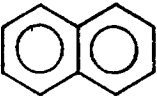
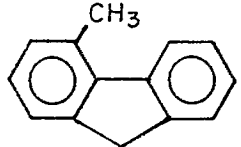
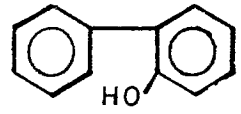
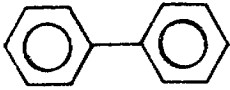
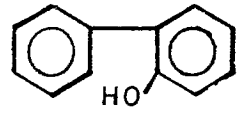
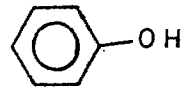
	HYDRO AROMATICS	AROMATICS	FURANS AND PHENOLS
4 RINGS		 0.38 PYRENE 0.38 METHYL PYRENE	
3 RINGS		 0.81 ANTHRACENE	 1.10 DIBENZOFURAN
2 RINGS	1.09 TETRAHYDRONAPHTHALENE 1.26 " METHYL " 1.09 " ETHYL "	 1.14 NAPHTHALENE 1.16 METHYL NAPHTHALENE 1.04 DIMETHYL NAPHTHALENE 1.06 ETHYL NAPHTHALENE 1.10 METHYL ETHYLNAPHTHALENE	 1.41 METHY FLUORENE 1.06 FLUORENE
			 1.02 METHYLDIBENZOFURAN
1 RING	1.43 BENZENE /CYCLOHEXANE 1.23 ETHYL CYCLOHEXANE	1.75 TOLUENE 1.49 ETHYL BENZENE 1.45 BUTHYL BENZENE 1.44 XYLENE 1.29 TRIMETHYL BENZENE 1.38 METHYL ETHYL BENZENE	 BIPHENYL 1.10 DIMETHYLBIPHENYL
			 BIPHENYL PHENOL
			 0.72 PHENOL 0.49 METHYL PHENOL 0.82 DIMETHYL BENZALDEHYDE

Table 4 - Pre-exponential factors and activation energies

	Empirical Factor-b	Pre-exponential Factors (s^{-1})	Activation Energy ($kJ\ mol^{-1}$)
Hydrodesulphurization	0	3.96	16.6
Hydrodenitrogenation	0	5.99×10^4	62.4
Hydrodeoxygenation	0.9	1.44×10^6	84.8

Table 5 - Surface composition of fresh catalyst,
used catalyst and ash from coal liquid
obtained by X-ray photoelectron spectroscopy

Component Atomic %	Atomic Per Cent		
	Fresh Catalyst	Used Catalyst	Ash from Coal Liquid
Zinc	-	0.9	29.5
Iron	-	-	1.4
Aluminum	16.9	8.3	-
Molybdenum	2.5	1.7	-
Cobalt	0.6	0.8	-
Carbon	36.7	59.3	28.1
Oxygen	43.4	25.7	38.6
Sulphur	-	3.3	2.5

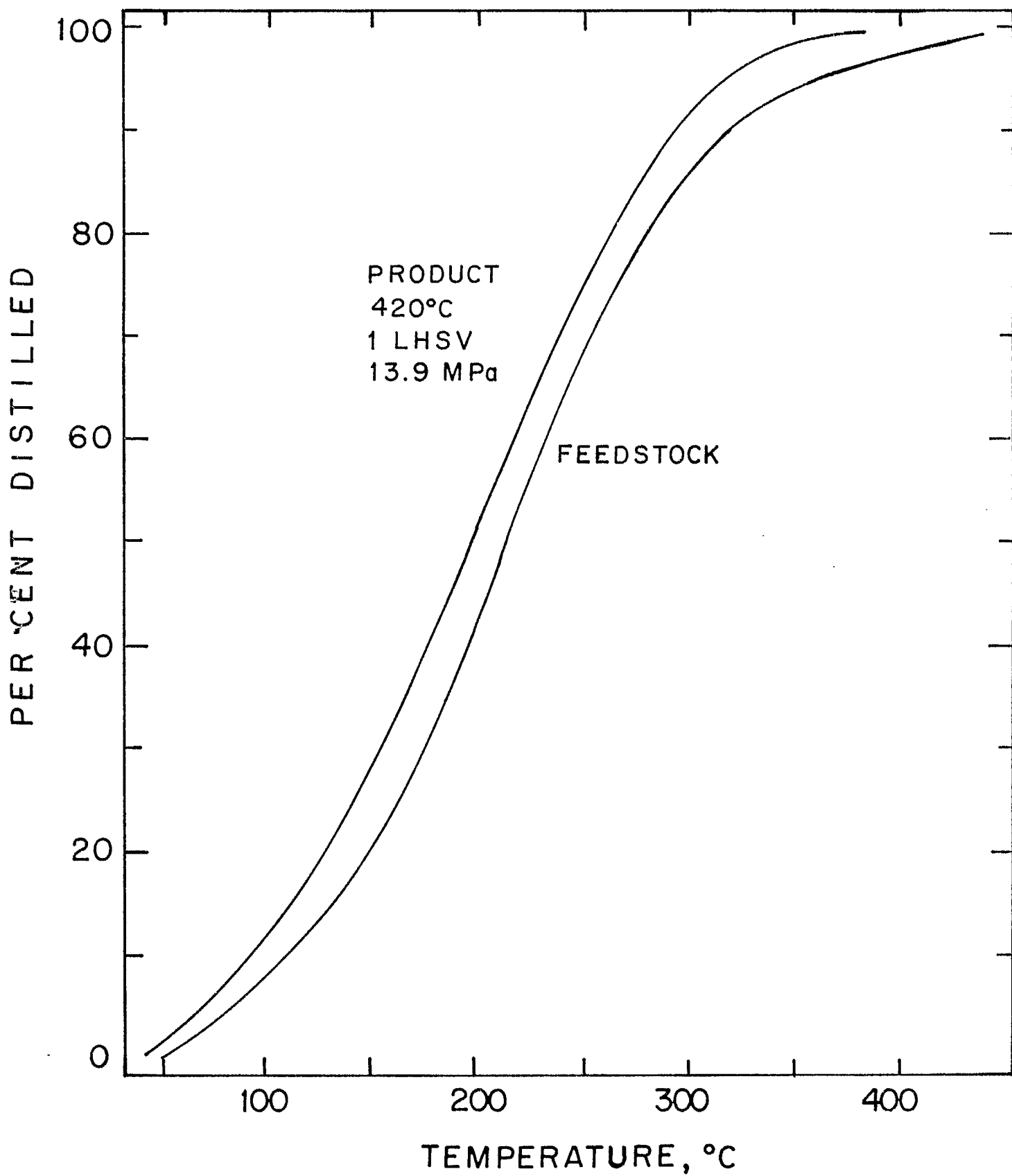


FIG 1

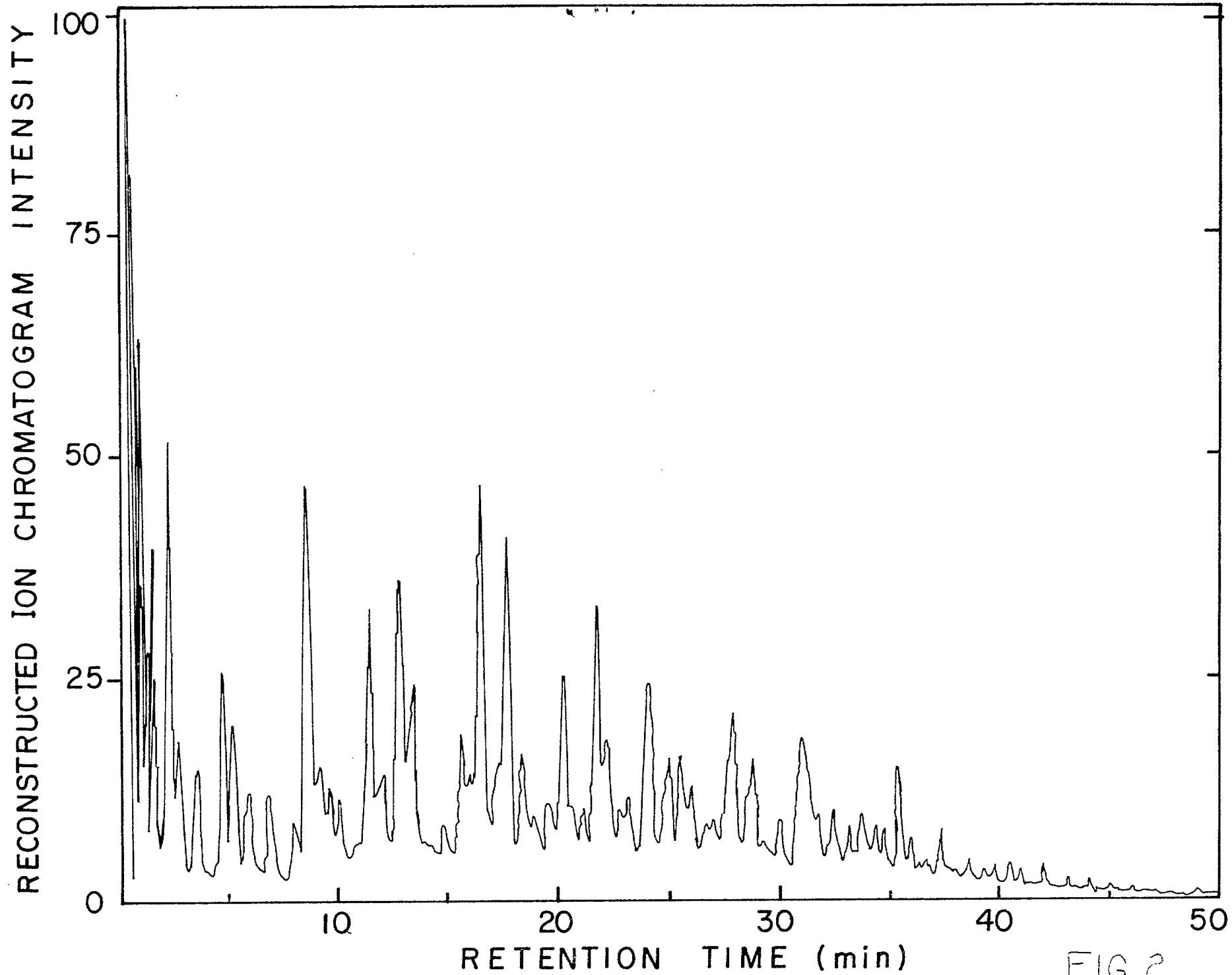


FIG 2

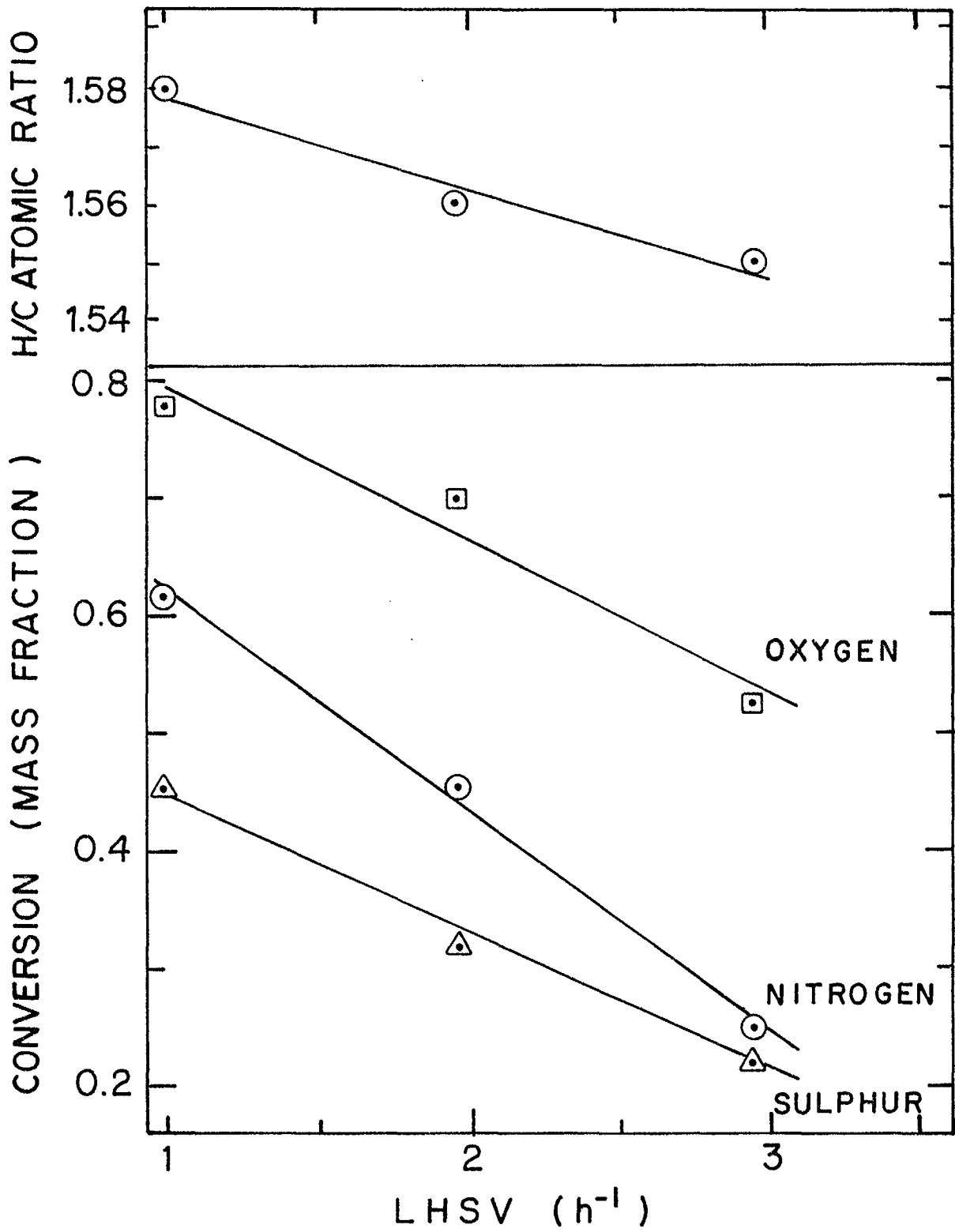


FIG 3

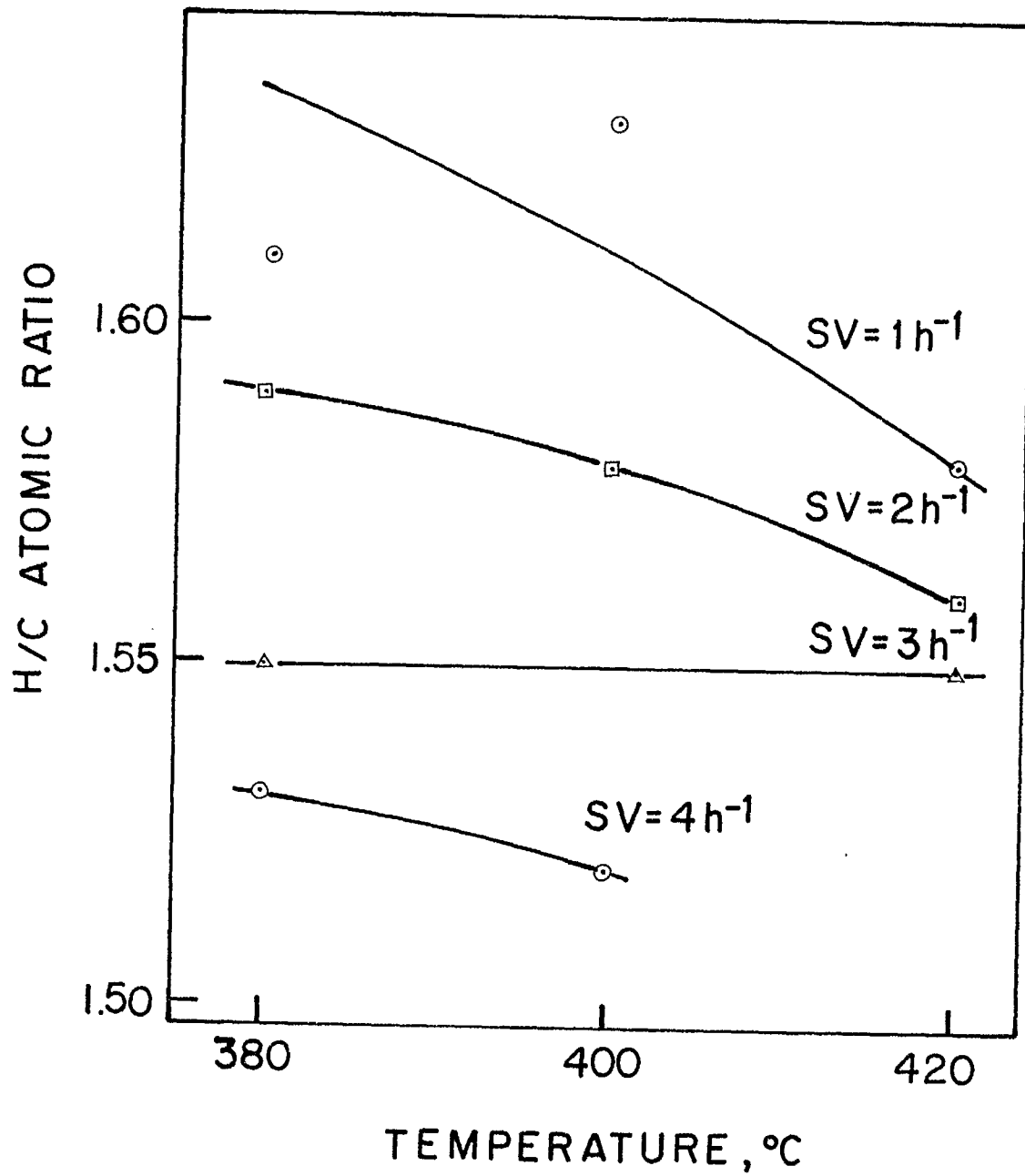


FIG 4

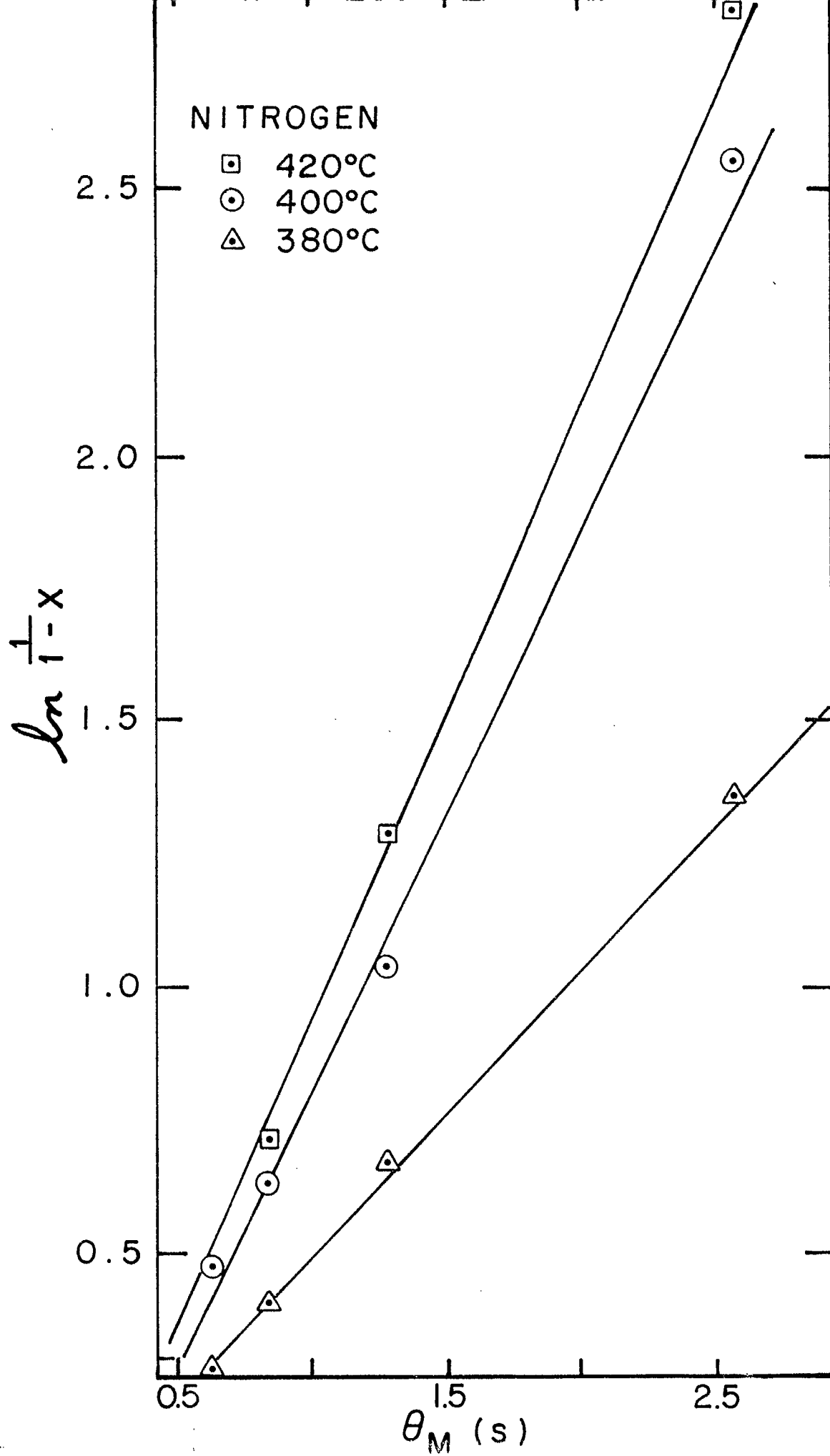


FIG 5

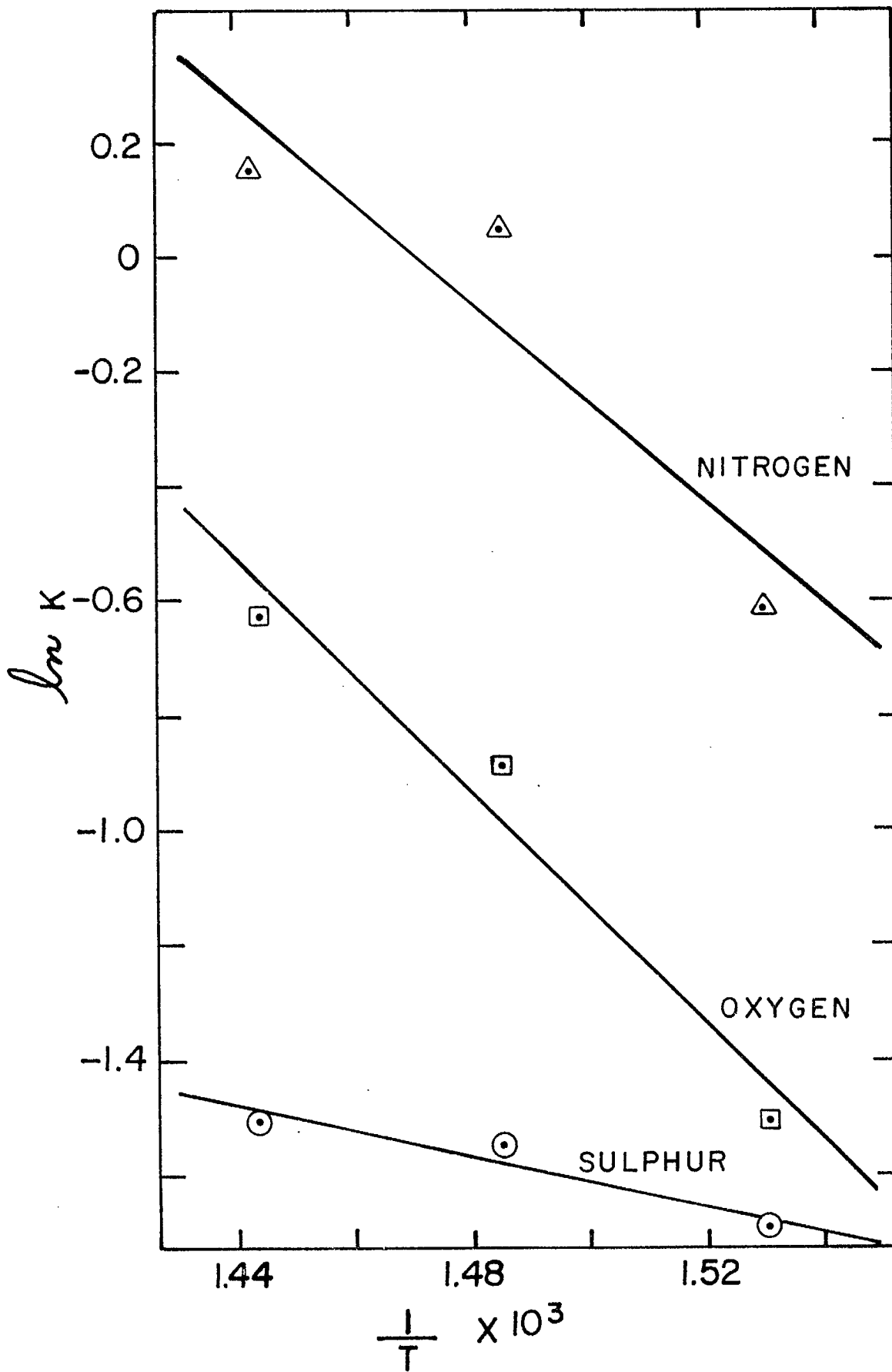


FIG 6

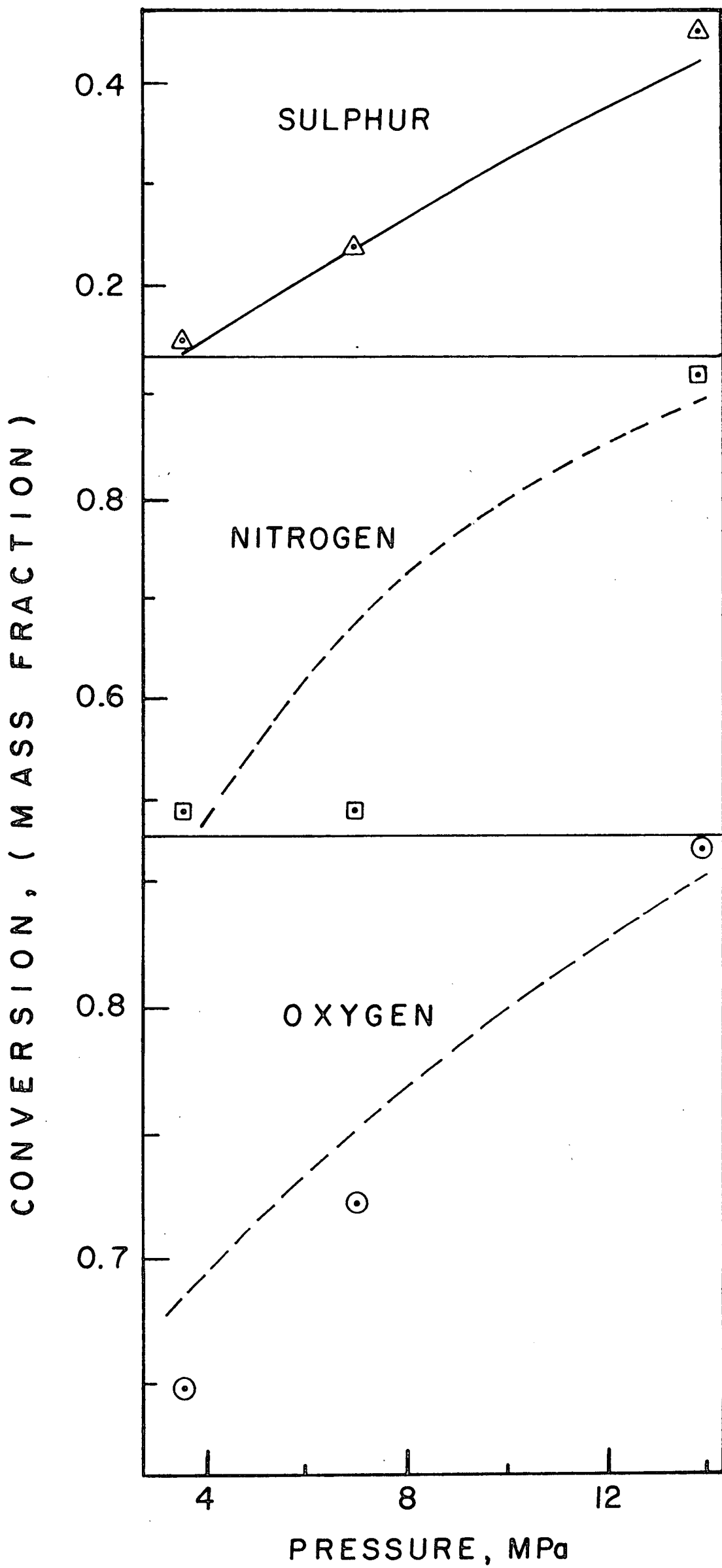


FIG 7

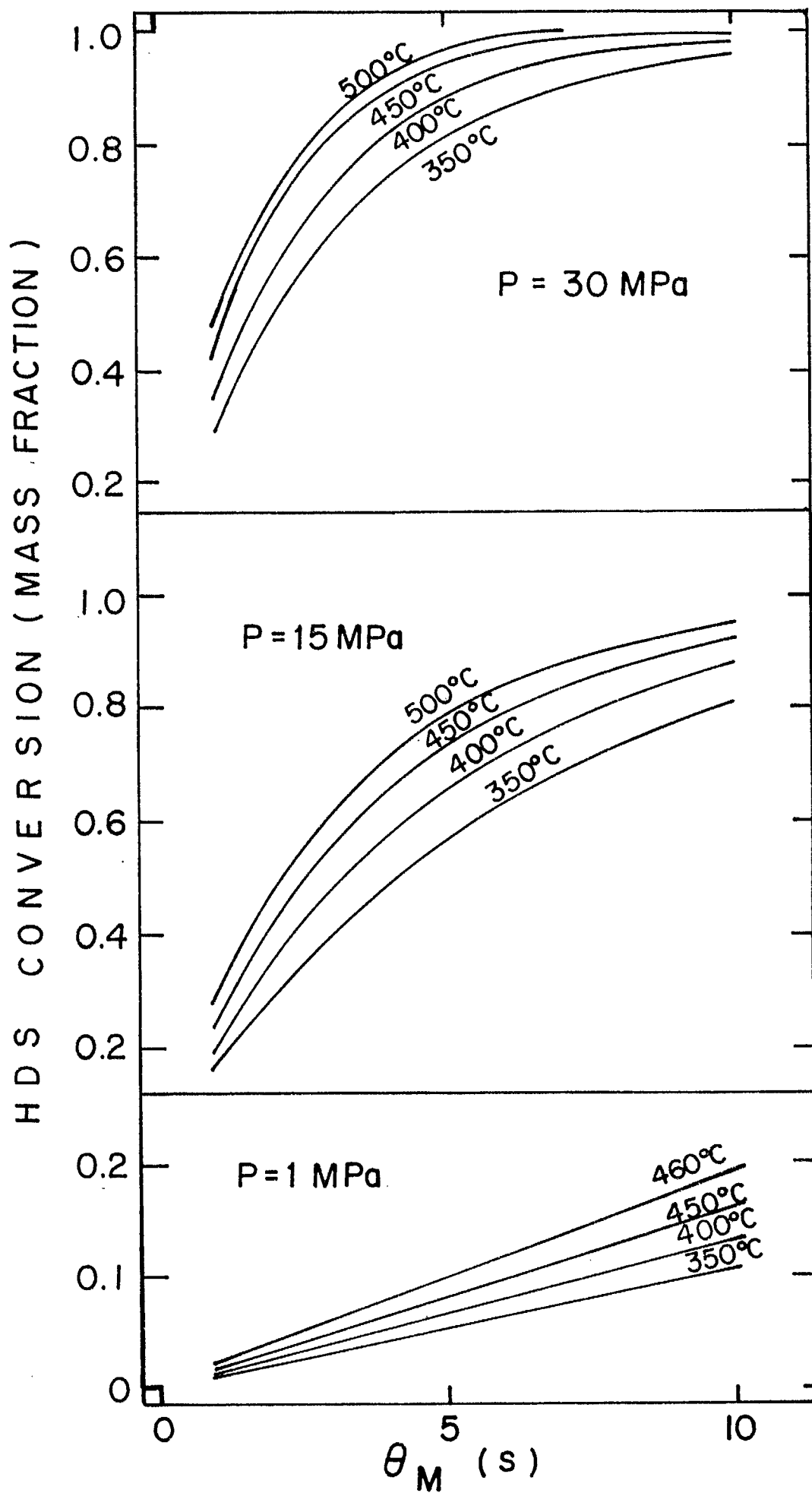


FIG 8

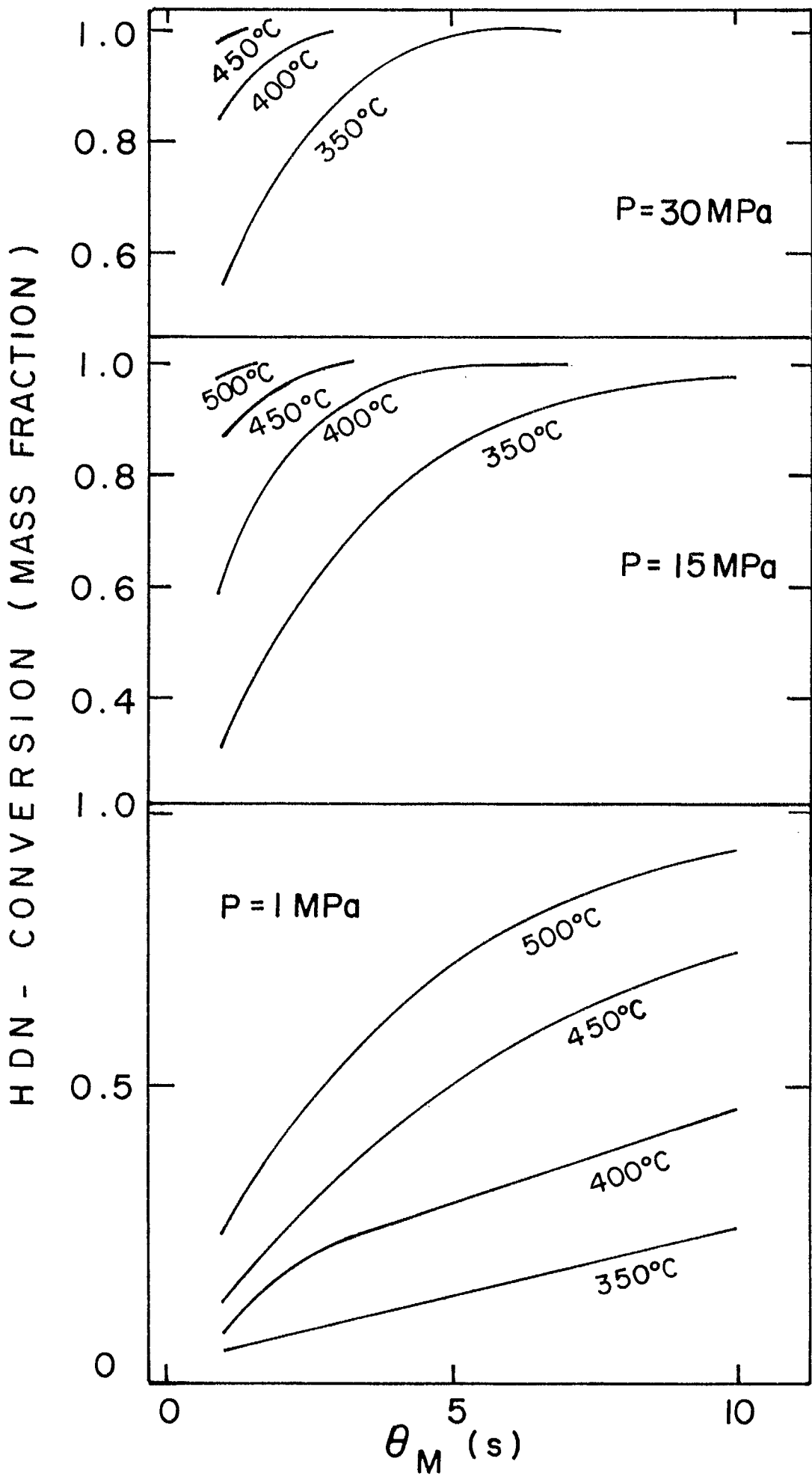


FIG 9

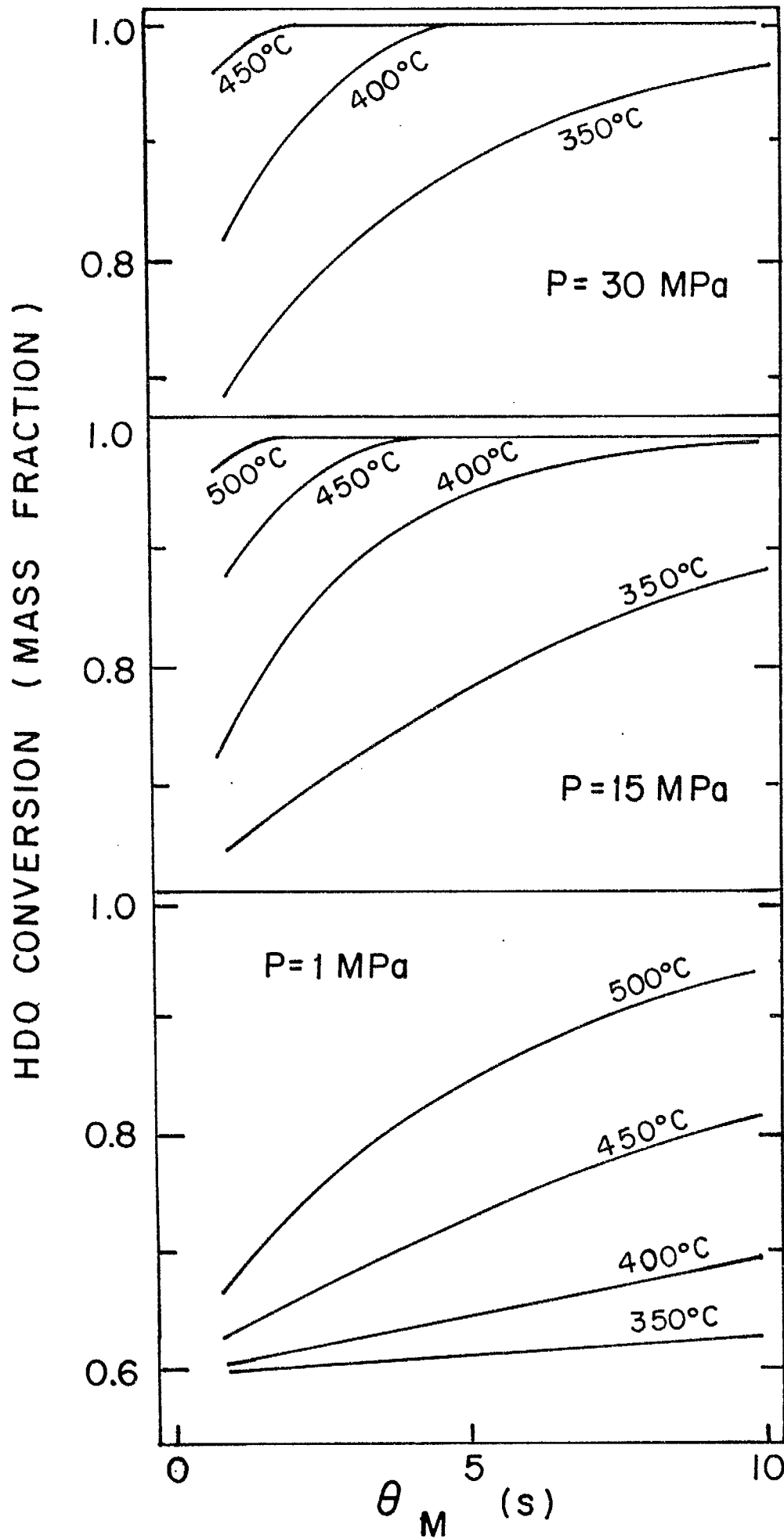


FIG 10

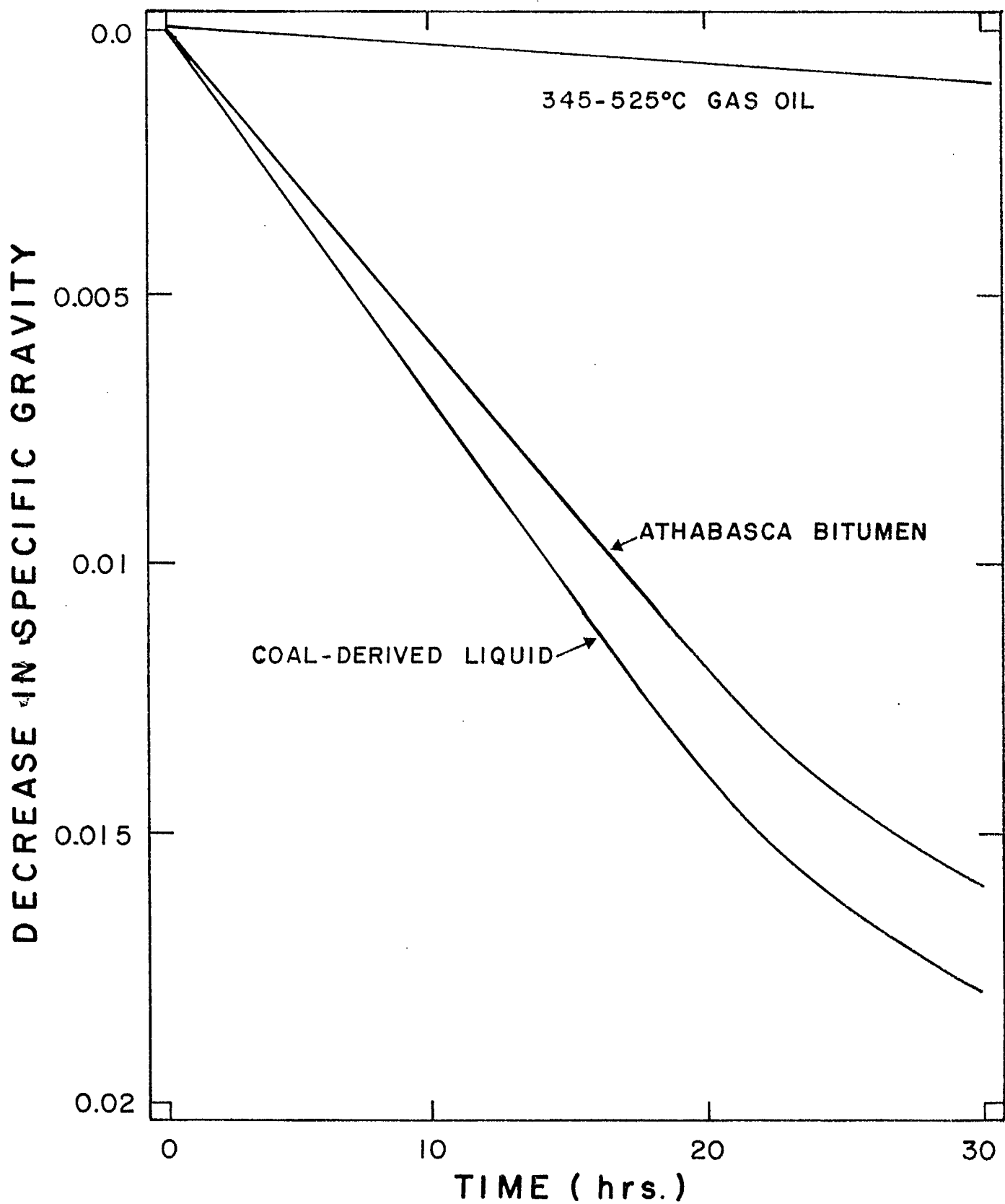


FIG 11